Functional histamine H_3 and adenosine A_{2A} receptor heteromers in recombinant cells and rat striatum

Ricardo Márquez-Gómez[a], Citlaly Gutiérrez-Rodelo[b], Meridith T. Robins[c], Juan-Manuel Arias[d], Jesús-Alberto Olivares-Reyes[b], Richard M. van Rijn[c] and José-Antonio Arias-Montaño[a]

Departamentos de [a]Fisiología, Biofísica y Neurociencias y [b]Bioquímica, Cinvestav-IPN, Av. IPN 2508, Zacatenco, 73063 Ciudad de México, México; [c]Department of Medicinal Chemistry and Molecular Pharmacology, Purdue University, West Lafayette, IN, USA; [d]Programa de Neurociencias-UIICSE, Facultad de Estudios Superiores Iztacala, UNAM, Av. de los Barrios 1, Los Reyes Iztacala, 54090 Estado de México, México

Corresponding author:

Dr. José-Antonio Arias-Montaño

Departamento de Fisiología, Biofísica y Neurociencias
Cinvestav-IPN
Av. IPN 2508, Zacatenco,
07360, Ciudad de México, México
Tel. (+5255) 5747 3964
Fax (+5255) 5747 3754
Email jaarias@fisio.cinvestav.mx

Abstract

In the striatum, histamine H_3 receptors (H_3Rs) are co-expressed with adenosine A_{2A} receptors (A_{2A}Rs) in the cortico-striatal glutamatergic afferents and the GABAergic medium-sized spiny neurons that originate the indirect pathway of the basal ganglia. This location allows H_3Rs and A_{2A}Rs to regulate the striatal GABAergic and glutamatergic transmission. However, whether these receptors interact to modulate the intra-striatal synaptic transmission has not yet been assessed. To test this hypothesis a heteromer-selective *in vitro* assay was used to detect functional complementation between a chimeric $A_{2A}R_{302}$-$G\alpha_{qi4}$ and wild-type H_3Rs in transfected HEK-293 cells. H_3R activation with the agonist RAMH resulted in Ca^{2+} mobilization (pEC_{50} 7.31 ± 0.23; maximal stimulation, Emax 449 ± 25 % of basal) indicative of receptor heterodimerization. This response was not observed with histamine, suggesting a RAMH bias for heteromers. Functional A_{2A}R-H_3R heteromers were confirmed by co-immunoprecipitation and observations of differential cAMP signaling when both receptors were co-expressed in the same cell. In membranes from rat striatal synaptosomes, H_3R activation decreased A_{2A}R affinity for the agonist CGS-21680 (pKi values 8.10 ± 0.04 and 7.70 ± 0.04). Moreover, H_3Rs and A_{2A}Rs co-immunoprecipitated in protein extracts from striatal synaptosomes. These results support the existence of a H_3R/A_{2A}R heteromer, and reveal a new mechanism by which these receptors may modulate the unction of the striatum and the basal ganglia.

Keywords

Adenosine A_{2A} receptor; histamine H_3 receptor; striatum; GPCR heterodimers; basal ganglia

1. Introduction

The actions of histamine in the periphery on airway constriction, inflammation and gastric acid secretion are well known, whereas its function in the Central Nervous System (CNS) is not yet fully understood. In mammals, histamine actions are mediated by four (H_1R-H_4R) G protein-coupled receptors (GPCRs), of which the H_3 receptor (H_3R) displays the highest expression in the brain. In the CNS histamine is released from the terminals and dendrites of neurons located in the hypothalamic tuberomammilary nucleus, from where they innervate most of the CNS, including nuclei belonging to the basal ganglia, a subcortical group of structures intimately related to the control of motor behavior (Panula and Nuutinen, 2013).

The striatum is the main input nucleus of the basal ganglia and integrates motor and sensory information. The primary striatal afferents are glutamatergic axons originating from neurons located in the cerebral cortex and thalamus, and dopaminergic axons of sustantia nigra pars compacta neurons (Bolam *et al*., 2000). In turn, the axons of the GABAergic medium-sized spiny neurons (MSNs), which account for more than 90% of the striatal neuronal cell population (Kemp and Powell, 1971), project to the globus pallidus and sustantia nigra pars reticulata (Bolam *et al*., 2000).

H_3Rs are abundantly expressed in the striatum either as pre-synaptic auto- and hetero-receptors or as post-synaptic receptors, with the latter located on the bodies of the MSNs and GABAergic or cholinergic interneurons (Pillot *et al*., 2002; González-Sepúlveda *et al*., 2013; Bolam and Ellender, 2016). The understanding of the physiological role of striatal H_3Rs is complicated by their ubiquitous expression and capability to engage in protein-protein interactions with other GPCRs (Nieto-Alamilla *et al*., 2016). Of particular interest

in the striatum are dopamine and adenosine receptors, which are also highly expressed. Based on the selective expression of dopamine and adenosine receptor subtypes, MSNs can be segregated into two neuronal populations. Neurons that originate the basal ganglia direct pathway (dMSNs) are identified by the expression of D_1 receptors (D_1Rs) whereas the indirect pathway population (iMSNs) is formed by neurons expressing adenosine A_{2A} receptors (A_{2A}Rs) and D_2 receptors (D_2Rs) (Schiffman *et al*., 1991; Ferre *et al*., 1997; Tapper *et al*., 2004). In the striatum H_3Rs have been shown to form heterodimeric protein-protein complexes with dopamine D_2-like and D_1-like receptors (Ellenbroek, 2013), and heterotrimers with $\sigma1/D_1$ receptors and NMDA/D_1 receptors (Moreno *et al*., 2014; Rodríguez-Ruíz *et al*., 2016). In turn, A_{2A}Rs can form dimers with D_2, cannabinoid CB_1 and adenosine A_1 receptors (Ciruela *et al*., 2006; Carriba *et al*., 2007; Hillon *et al*., 2002) and oligomers with D_2 and mGlu5 glutamate receptors (Cabello *et al*., 2009).

Both H_3 and A_{2A} receptors modulate intra-striatal synaptic transmission. The activation of $G\alpha_{i/o}$-coupled H_3Rs results in inhibition of GABA, dopamine, acetylcholine and glutamate release (Doreulee *et al*., 2001; Schlicker *et al*., 1993; Prast *et al*., 1999; Arias-Montaño *et al*., 2001), whereas the activation of $G\alpha_{olf}$-coupled A_{2A}Rs also inhibits GABA release but facilitates glutamatergic cortico-striatal transmission (Kirk and Richardson, 1994; Popoli, 1995).

Either individually or through their heteromeric interactions with other GPCRs, A_{2A}Rs and H_3Rs have been proposed as targets for the treatment of basal ganglia-related disorders such as Parkinson's disease and addiction (Ferré *et al*., 2004; Schwarzschild *et al*., 2006; Passani and Blandina, 2011; Ellenbroek, 2013). In this work, we hypothesized that striatal H_3Rs and A_{2A}Rs can not only form heteromers with dopamine receptors, but also with each

other, and that this interaction forms a unique pharmacological target that could be of potential therapeutic interest. Here we show that H_3Rs co-immunoprecipitate with A_{2A}Rs in HEK293 cells, suggestive of oligomerization. Further, we studied the physical properties of the $A_{2A}R/H_3R$ interaction by functional complementation assay, in which we found an intriguing example of biased agonism. We next show that the $A_{2A}R/H_3R$ heteromerization has unique functional pharmacology in terms of cAMP modulation in HEK-293 cells co-expressing the receptors. Using protein extracts from striatal synaptosomes, we confirmed the presence of $A_{2A}R/H_3R$ heteromers *in vivo* by co-immunoprecipitation. Finally, we found that in the same preparation H_3R activation resulted in decreased binding affinity of $A_{2A}R$ for the agonist CGS-21680.

A preliminary account of this work was presented in the abstract form to the European Histamine Research Society (Márquez-Gómez et al., 2016).

2. Methods

2.1 Materials

The following drugs and reagents were purchased from Sigma Aldrich (St. Louis, MO, USA): (R)-α-methyl-histamine dihydrochloride, histamine dihydrochloride, adenosine deaminase (from bovine spleen), Percoll, quinpirole dihydrochloride and caffeine. Dimaprit was from Axon MedChem (Reston, VA, USA). CGS-21680 was from Cayman Chemical (Ann Arbor, MI, USA). N-α-[methyl-^{3}H]-histamine (78.3 Ci·mmol^{-1}) and CGS-21680-[carboxyethyl-^{3}H (N)]-(35.2 Ci·mmol^{-1}) were from Perkin Elmer (Boston, MA, USA).

2.2 Molecular cloning

Truncated A_{2A} or H_3 receptors were generated by PCR using the primers indicated in Supplementary Table 1. After amplification and restriction with HindIII and BamHI enzymes, the truncated A_{2A} and H_3 receptors were ligated to a pcDNA3.1 plasmid that contained the chimeric $G\alpha_{qs4}$ and $G\alpha_{qi4}$ proteins. Both A_{2A}Rs and H_3Rs (cDNA Resource Center, Bloomsberg, PA, USA) were labeled with a triple hemagglutinin tag (3xHA). To generate the 3xHA tagged receptors, A_{2A}R and the H_3R were amplified from nucleotide 377 and 458, respectively, towards their amino terminus. The 3xHA tag was amplified from a plasmid that codified for the tagged histamine H_4R (3xHA-H_4R in pcDNA3.1, cDNA Resource Center). The amplified DNA fragments (3xHA-A_{2A}R377/H_3R458) where then re-introduced into the pcDNA3.1-H_3R or pcDNA3.1-A_{2A}R backbone to obtain the tagged, full length receptors. The insertion and orientation of the amplified fragment was verified by automated sequencing performed at FESI-UNAM (Los Reyes Iztacala, Estado de México, México).

2.3 Cell culture and transfection

HEK-293T cells (American Type Culture Collection, Manassas, VA, USA) were grown in Dulbecco's modified Eagle's medium (DMEM) supplemented with 10% fetal bovine serum (FBS), penicillin (50 UI/ml) and streptomycin (0.1 mg/ml) under a humidified atmosphere (5% CO_2 in air) at 37 °C.

For transfections, cells were seeded in 6-well plates ($6x10^5$ cells/well; up to passage 15) and incubated for 24 h at 37 ºC in a 5% CO_2/air mixture. The next day, 10 µl X-tremeGENE (Roche, Basilea, Switzerland) were mixed with 500 µl Optimem (Life Technologies, San Diego, CA, USA) and the mixture was incubated for 5 min at room temperature before the addition of cDNA in a 1:5 ratio with X-tremeGENE. For cAMP assays a mixture of DNA:Glosensor cAMP plasmid (1:2 ratio) was added to the Optimem/X-tremeGENE solution. When plasmids containing the $A_{2A}R$ or H_3R were transfected alone, the amount of DNA was preserved by adding empty pcDNA3.1 vector. The transfection mixture was incubated for 20 min at room temperature and then added to the cells, which were incubated for 24 h at 37 ºC under a humidified atmosphere (5% CO_2/air).

For co-immunoprecipitation assays, HEK-293 cells, grown in 100-millimeter Petri dishes and at 80% confluence, were transfected using the polyethylenimine (PEI) method. Briefly, a mixture of DNA/PEI (1:10 ratio) was incubated for 30 min at room temperature before being added to the cells. After incubation for 30 min at 37 °C under a humidified atmosphere (5% CO_2/air), cells were supplemented with 10% FBS and incubation continued for further 24 h under the same condition.

2.4 cAMP accumulation assay

cAMP assays were performed as described in detail elsewhere (Chiang et al. 2016). Briefly, HEK-293 cells transfected with 3xHA-A_{2A}R, 3xHA-H_3R or a mixture of both plasmids (1 µg each) together with Glosensor cAMP plasmid (Promega, Madison, WI, USA) were seeded in a white 384-well low-volume plate (25,000 cells/well in 7.5 µl medium) and incubated with Glo-equilibrium medium (7.5 µl, Promega). Drugs under test were added in a 5 µl volume (4x in HBSS solution) and endogenous cAMP luminescence was measured in real-time in a Flexstation 3 apparatus (Molecular Devices, Sunnyvale, CA, USA).

2.5 Calcium mobilization assay

HEK-293T cells transfected with 1 µg of DNA were seeded ($2.5x10^4$ cells/well) in a 384-well clear bottom black plate (25 µl-volume) and incubated for 24 h at 37 ºC in a humidified 5% CO_2/air atmosphere, covered with Areaseal film (Sigma, St. Louis, MO, USA). Cells were then loaded with 25 µl of the FLIPR Ca^{2+} dye (Molecular Devices, Sunnyvale, CA, USA) and incubated for 1 h at 37 ºC. Agonists were added in a 20 µl volume and calcium mobilization was measured in real-time for 2 min in a Flexstation 3 apparatus (Molecular Devices, Sunnyvale, CA, USA) and analyzed as described in detail in van Rijn *et al*. (2013).

2.6 Synaptosome preparation

Wistar rats (males, 250-300 g, provided by the Unidad de Producción y Experimentación para Animales de Laboratorio; UPEAL-Cinvestav, Mexico City) were decapitated and the brain was quickly removed from the skull and the forebrain was separated and deposited on a metal plate placed on ice. The striata from 3-5 animals were dissected using forceps and

the tissue was placed in 5 ml 0.32 M sucrose solution containing 10 mM Hepes, 1 mg/ml bovine serum albumin and 1 mM EDTA (pH 7.4 with NaOH). The tissue was homogenized using 10 strokes of a hand-held homogenizer (400 rpm), the homogenate was centrifuged (1000x*g*, 10 min, 4 °C) and the supernatant was pelleted at 14,000x*g* (12 min, 4 °C). The pellet was re-suspended in 5 ml of a Percoll solution (45 %, v:v), in Krebs-Henseleit-Ringer buffer (in mM: NaCl 140, Hepes 10, D-glucose 5, KCl 4.7, EDTA 1, pH 7.3 with NaOH). After centrifugation (2 min, 14,000x*g*, 4 °C), the upper phase was collected and brought up to 20 ml with Krebs-Ringer-Hepes (KRH) solution (in mM: NaCl 113, $NaHCO_3$ 25, Hepes 20, D-glucose 15, KCl 4.7, $CaCl_2$ 1.8, $MgCl_2$ 1.2, KH_2PO_4 1.2, pH 7.4 with NaOH). The suspension was centrifuged (20,000x*g*, 20 min, 4 °C) and the pellet (synaptosomes) was re-suspended in KRH solution unless otherwise indicated.

2.7 Electron microscopy

Striatal synaptosomes were isolated by the Percoll method as above. Sample preparation and electron microscopy were performed as described in detail elsewhere (Morales-Figueroa *et al.*, 2015).

2.8 Radioligand binding assays with striatal membranes

Striatal synaptosomes were re-suspended in lysis solution (Tris-HCl 10 mM, EGTA 1 mM, pH 7.4) and incubated for 20 min at 4 ºC before centrifugation (20 min, 20,000xg, 4 ºC). The pellet (synaptosomal membranes) was re-suspended in 1 ml KRH solution containing adenosine deaminase (2 U/ml). After incubation for 30 min at 37 ºC, the suspension was brought to 20 ml with KRH solution and centrifuged (20 min, 20,000x*g*, 4 ºC), the membranes were re-suspended in incubation solution (Tris-HCl 50 mM, $MgCl_2$ 5 mM, pH 7.4) and 130 µl aliquots (300 µg protein) were incubated with 10 µl of increasing

concentrations of CGS-21680 or RAMH (20x) and 50 µl of a fixed concentration of [^{3}H]-NMHA (8 nM) or [^{3}H]-CGS-21680 (48 nM). After 1 h at 30 ºC ([^{3}H]-NMHA) or 2 h at 25°C ([^{3}H]-CGS-21680), incubations were stopped by rapid filtration through Whatman GF/B filters pre-soaked (2 h) in 0.3 % polyethylenimine (PEI). Filters were washed 3 times with 1 ml ice-cold buffer solution (50 mM Tris-HCl, pH 7.4), soaked in 4 ml scintillation solution and the tritium content was determined by scintillation counting.

2.9 Co-immunoprecipitation assays

Striatal synaptosomes were obtained as described above and then re-suspended in 1 ml of lysis solution (Tris-HCl 50 mM, NaCl 150 mM, Triton X-100 1%, SDS 0.05%, protease inhibitor 1 µl/ml). HEK-293 cells were dislodged in RIPA solution. For both synaptosomal and cell samples, protein was extracted by sonication (3 cycles, 30 sec, 8 kHz). The sample was centrifuged (20 min, 6,000x*g*) and the protein extract (supernatant) was collected. Nonspecific binding was removed by incubation (1 h, 4 ºC) with 10 µl of AG beads (Santa Cruz Biotechnology; Dallas, TX, USA) under rotatory rocking. The beads were pelleted (2 min, 6000x*g*) and the supernatants were used for the assay. Protein quantification was performed by the BCA method.

The protein extracts (500 µg protein from striatal synaptosomes and 200 µg from HEK-293) were incubated with 2 µg of the primary antibodies (anti-A_{2A}R abcam, cat. ab3461, lot. GR238882-9; anti-HA, Cell Signaling, cat. C29F4, lot. 3724S; anti-H_3R, abcam, cat. ab84468, lot. GR27494-1, in a 1:100 dilution) together with AG beads (Santa Cruz Biotechnology sc-2003, 1:5 antibody to beads ratio) for 16 h at 4 ºC with constant rotational rocking. Antibodies against the CD-81 protein (Santa Cruz Biotechnology, cat. sc-70803, lot. B0609) or D_2R (Santa Cruz Biotechnology, cat. sc-5303, lot. A03013) were

used as negative controls for the striatal synaptosomes or HEK-293 cells, respectively. The bead-antibody complex was pelleted (2 min, 6000x*g*) and a 30 µl aliquot of the supernatant was used as a load control. In both protein extracts, 30 µl of the total protein was used as input. The complex was dissociated for 60 min at 48ºC in loading buffer (10% β-mercaptoethanol and 50% Laemmli buffer in H_2O,) and separated by electrophoresis on a 10% SDS-polyacrylamide gel (20 min at 80 V and then 65 min at 120 V). Semi-dry transfer was performed at 15 V for 95 min. Membranes were blocked with 5% nonfat dry milk diluted in TBS-Twin 0.05% solution (overnight, 4 ºC). After extensive washing, 5 ml of TBS-Twin 0.05% solution containing 5% BSA and the blotting antibody (anti-$A_{2A}R$, anti-HA or anti-H_3R, in a 1:1000 dilution) were added to the membrane and incubated overnight at 4 ºC. Membranes were incubated with the secondary antibody (Invitrogen, HRP-conjugated anti-rabbit IgGs, cat. 65-6120, 1:5000, non-fat dry milk 5% in TBS-Twin 0.05%) at room temperature for 2 h. For the loading controls membranes were incubated for 1h with antibodies directed to β-tubulin (Invitrogen, cat. 322600, lot. 1235662) or α-actin (Sigma, cat. A5228, lot. 128K4843) in a 1:5000 dilution in TBST 0.05%. After washing, membranes were incubated for 1 h with the secondary antibody (α-mouse, Santa Cruz, cat. sc-2005) diluted in TBST 0.05%. Blot images were obtained by chemiluminescence in an X-ray film (Kodak).

2.10 Statistical analysis

All data was analyzed using the Prisma GraphPad software (San Diego, CA, USA). Data shows mean ± standard error of the mean (SEM). Statistical analysis was performed with student *t*-test.

3 Results

3.1 Co-immunoprecipitation of A_{2A}Rs and H_3Rs expressed in HEK-293 cells

In order to provide biochemical evidence for the hypothesized heteromerization of H_3Rs and A_{2A}Rs, we first studied by co-immunoprecipitation whether H_3Rs and A_{2A}Rs interact physically upon co-transfection in HEK-293 cells. The 3xHA-H_3Rs were detected after immunoprecipitation of WT-A_{2A}R (Figure 1A). No signal was observed when an antibody against the D_2R (α-D_2R) was employed as a negative control. These results support dimerization between H_3Rs and A_{2A}Rs.

3.2 Functional complementation of A_{2A}Rs and H_3Rs expressed in HEK-293 cells

To further study the potential interaction between A_{2A}Rs and H_3Rs in a recombinant cell system we employed a functional complementation assay, previously used to study physical interactions between GPCRs (Han *et al.*, 2009; van Rijn *et al.*, 2013). This assay relies on the fusion of chimeric $G\alpha_{qs4}$ or $G\alpha_{qi4}$ proteins to the truncated C-terminal tail of a GPCR to generate a nonfunctional receptor, rescuable through homo- or hetero-dimerization with a wild type (WT), untruncated receptor. It was previously reported that fusion of a chimeric G protein to a GPCR truncated near helix 8 produces a receptor that is unable to signal by itself but can be rescued when transfected with a full length receptor (van Rijn *et al*., 2013). Therefore, we first generated an A_{2A}R truncated to 302 residues ($A_{2A}R_{302}$) and H_3Rs of 427, 421 and 411 residues (H_3R_{427}, H_3R_{421} and H_3R_{411}), and the truncated receptors were then fused to the chimeric G proteins (Figure 2A).

Activation of the H_3R in transfected CHO-K1 cells and rat striatal neurons in primary culture induces Ca^{2+} mobilization (Cogé *et al*., 2001; Rivera-Ramirez *et al.*, 2016), and in the striatum $A_{2A}R$ activation favors Ca^{2+} entry by modulating voltage-activated Ca^{2+} channels (Kirk and Richardson, 1995; Gubitz *et al.*, 1996), which are endogenously expressed by HEK-293 cells (Berjukow *et al.*, 1996; Thomas and Smart, 2005). In HEK-293 cells the H_3R selective agonist RAMH did not induced any discernible Ca^{2+} response but did so when the H_3R was co-transfected with $G\alpha_{qi4}$ proteins (Figure 2B). The $A_{2A}R$ did not induce Ca^{2+} signaling when activated by the selective agonist CGS-21680, but also no response was observed when co-transfected with $G\alpha_{qs4}$ proteins, suggesting that $A_{2A}Rs$ do not activate this chimeric protein (Figure 2C). It has been reported that not all GPCRs are amenable to signal through chimeric G-proteins (Conklin *et al.*, 1996). A different $G\alpha_s$-coupled receptor, the histamine H_2 receptor, was capable to induce calcium release when co-transfected with $G\alpha_{qs4}$ proteins and stimulated with the selective agonist dimaprit (Supplementary Figure 1A), discarding $G\alpha_{qs4}$ malfunction. Consistent with the finding that $A_{2A}Rs$ did not signal efficiently via chimeric G-proteins, functional complementation by homodimerization of $A_{2A}R_{302}$-$G\alpha_{qs4}$ or $A_{2A}R_{302}$-$G\alpha_{qi4}$ with the full length $A_{2A}R$ was not observed (Figure 2D).

The C-tail of the H_3R was truncated such that the H_3R-$G\alpha_{qi4}$ fusion protein would display limited Ca^{2+} mobilization when expressed alone, but pronounced Ca^{2+} signaling when co-expressed with WT-H_3Rs. The H_3R_{421}-$G\alpha_{qi4}$ and the H_3R_{411}-$G\alpha_{qi4}$ constructs did not induce Ca^{2+} mobilization, and could not be rescued via homo-dimerization with WT-H_3Rs (Supplementary Figure 1B). However, Ca^{2+} mobilization induced by H_3R_{427}-$G\alpha_{qi4}$ upon activation and co-transfection with WT-H_3Rs produced a similar increase in calcium

release (Figure 2E). While not optimal, this behavior allowed for the study of the interaction between the H_3R_{427}-$G\alpha_{qi4}$ and the $A_{2A}R$ as explained below.

Co-transfection of the 'inert' $A_{2A}R_{302}$-$G\alpha_{qi4}$ and H_3Rs induced Ca^{2+} mobilization after activation of the latter receptors with RAMH, suggestive of close physical proximity between the H_3R and both the $A_{2A}R$ and the fused $G\alpha_{qi4}$-protein. H_3R activation failed to induce functional complementation in cells co-transfected with $A_{2A}R_{302}$-$G\alpha_{qs4}$ (Figure 3A). Given that H_3Rs are $G\alpha_{i/o}$-coupled, and the inability of the $A_{2A}R$ to signal through chimeric $G\alpha_{qi4}$- or $G\alpha_{qs4}$-proteins, it was not surprising that $A_{2A}R$ activation with the selective agonist CGS-21680 did not produce any response through H_3R_{427}-$G\alpha_{qs4}$ or H_3R_{427}-$G\alpha_{qi4}$ (Figure 3B). Interestingly, the co-expression of WT $A_{2A}Rs$ prevented RAMH-induced calcium mobilization mediated by the H_3R_{427}-$G\alpha_{qi4}$ (compare Figure 2E and Figure 3C). We briefly explored this pharmacological response further by analyzing calcium release in HEK-293 cells co-expressing the H_3R_{427}-$G\alpha_{qi4}$ and the $A_{2A}R$ or the $A_{2A}R_{302}$-$G\alpha_{qi4}$ and the H_3R and activating both receptors, but did not observe any additive or antagonistic effect (Supplementary Figure 1C and 1D).

$A_{2A}Rs$ have been shown to form heteromers with D_2Rs (Ferré *et al.*, 2003) and robust functional complementation was accordingly observed when $A_{2A}R$-$G\alpha_{qi4}$ was co-expressed with WT-D_2Rs (Figure 3D), supporting that our results are due to heterodimerization and not to stochastic interactions.

3.3 The putative $A_{2A}R/H_3R$ heteromer displays ligand bias

To test for the selective nature of the $A_{2A}R/H_3R$ interaction in the functional complementation assay, we investigated if $A_{2A}R$-$G\alpha_{qi4}$ would also allow the structurally and physiologically similar histamine H_4 receptor (H_4R) to induce calcium release. Co-activation with histamine of H_3Rs and H_4Rs elicited Ca^{2+} mobilization only when co-transfected with $G\alpha_{qi4}$ (Supplementary Figure 2A and 2B, respectively). Neither histamine nor RAMH induced Ca^{2+} release when the H_4R was co-expressed with $A_{2A}R_{302}$-$G\alpha_{qi4}$, supporting the specificity of the $A_{2A}R/H_3R$ interaction (Figure 3E). Unexpectedly, whereas RAMH induced Ca^{2+} mobilization when the H_3R was co-expressed with $A_{2A}R_{302}$-$G\alpha_{qi4}$, histamine did not (compare Figure 3A with Figure 3F). This result suggests that the $A_{2A}R/H_3R$ heteromer displays agonist bias.

3.4 $A_{2A}R$-mediated signaling is increased by H_3R co-activation

To study the pharmacology of the putative $A_{2A}R/H_3R$ heteromer we next tested cAMP signaling using WT receptors in HEK-293 cells. In cells transfected with $A_{2A}Rs$, incubation with CGS-21680 resulted in a concentration-dependent increase in cAMP levels in accordance with the receptor's coupling to the $G\alpha_s$ signaling pathway (Figure 3A). CGS-21680 induced a similar cAMP response in HEK293-$A_{2A}R$ cells co-expressing H_3Rs (Figure 4A). Co-activation of the receptors resulted in a decrease in baseline, in accordance with the $G\alpha_{i/o}$ coupling of the H_3R, but led to an augmentation of $A_{2A}R$-mediated cAMP formation as noticed by a 2.5 fold change over baseline (versus 1.5 fold in control). This result suggests that the $A_{2A}R$ signaling becomes more efficacious when heterodimerization with the H_3R occurs (Figure 4A, Supplementary Figure 2C, and Table 2). The increase in

the $A_{2A}R$ signaling was not observed in the absence of RAMH (1.5 fold over baseline) suggesting an agonist-dependency of the response (Figure 4A and Supplementary Figure 2C).

In HEK293-H_3R cells RAMH inhibited forskolin-stimulated cAMP formation congruent with the $G\alpha_{i/o}$ coupling of the receptor. However, when the $A_{2A}R$ was co-transfected, RAMH-mediated H_3R signaling shifted to facilitate cAMP formation instead. Activation of the $A_{2A}R$ caused an expected increase in the baseline but it did not significantly modify the cAMP-increase effect. This result suggests that in the heterodimer, $A_{2A}R$ signaling prevails over the H_3R (Figure 4B; Table 2).

3.5 H_3R activation decreases $A_{2A}R$ binding affinity in synaptosomal membranes

The identification of $A_{2A}R/H_3R$ heteromers was performed in recombinant cell systems over-expressing the receptors. As previously mentioned $A_{2A}Rs$ and H_3Rs are co-expressed in iMSNs and cortico-striatal projections. We therefore used rat striatal synaptosomes to seek for pharmacological traces that supported the existence of native $A_{2A}R/H_3R$ dimers.

Electron microscopy confirmed in the purified synaptosomal preparation the vast presence and conserved structure of isolated nerve terminals, characterized by a delimited membrane and the presence of mitochondria and synaptic vesicles (Supplementary Figure 3A and B). In protein extracts from striatal synaptosomes immunoprecipitation of the $A_{2A}R$ resulted in a band of ~45 kDa, corresponding to the expected migration of the H_3R. No signal was detected when an irrelevant antibody (α-CD81) was tested. As a positive control the H_3R was immunoprecipitated and detected as a band of the same 45 kDa (Figure 5A). When the reverse approach was employed and the H_3R was immunoprecipitated from the striatal

protein extracts, a band of ~45 kDa corresponding to the expected migration of the $A_{2A}R$ was observed. This band was also observed when the $A_{2A}R$ was immunoprecipitated as a positive control but not detected in the negative control (Figure 5B). This result supports that the interaction $A_{2A}R/H_3R$ is constitutively present in the striatal nerve terminals.

In binding studies with synaptosomal membranes the $A_{2A}R$ agonist CGS-21680 (10 and 100 nM) did not affect the affinity of the H_3R for its agonist RAMH (Figure 5C), whereas RAMH (100 nM) decreased by two-fold the affinity of the $A_{2A}R$ for CGS-21680 (Figure 5D, 5E and Table 3), with no effect on maximal binding (Bmax). This pharmacology appears to be specific for pre-synaptic H_3Rs and $A_{2A}Rs$, because we did not observe a similar decrease in $A_{2A}R$ affinity for CGS-21680 in membranes from the whole striatum, in which post-synaptic membranes constitute the major component (Figure 5F and Table 3).

4 Discussion

The H_3R has been proposed as a potential novel drug target for the treatment of drug use disorders, depression, schizophrenia and Parkinson's disease. However, its wide brain expression and effects on other neurotransmitter systems may result in adverse effects when H_3R selective drugs are administered systemically. The $A_{2A}R$ has also been proposed as an option for the treatment of Parkinson´s disease and possesses a strategic distribution in the striatum for targeting and modulating the cortico-dMSNs projections and the activity of iMSNs. The results presented herein may lead to an alternative to specifically target H_3Rs located in either iMSNs or cortical afferents synapsing onto dMSNs projections.

4.1 $A_{2A}R/H_3R$ interaction

The primary finding of this study was the identification, for the first time, of $A_{2A}R/H_3R$ heteromers, not only in recombinant cell systems but also in rat striatal nerve terminals.

The basis of the functional complementation assays requires for a receptor to be nonfunctional and this was obtained by truncation of the carboxyl terminus (CT). Herein we showed that truncation of the H_3R from 445 to 411 or 421 residues was sufficient to prevent H_3R-mediated G protein activation of the H_3R-G_{qi4} fusion protein, yet we were unable to functionally rescue signaling, indicating that the remaining C-tail may be too short to connect with an interacting GPCR. However, truncation to 427 amino acids allowed the H_3R to remain functional. It may be possible to create a truncated version of the H_3R somewhere between amino acids 421-427 short enough to abolish homo/monomeric signaling but long enough to functionally complement with a full length GPCR. A requirement for helix 8 has been demonstrated for D_1Rs and opioid κ and μ

receptors (van Rijn *et al*. 2013). The H_3R third intracellular loop appears to play a key role in the receptor-G protein coupling on the basis of the decreased signaling of the H_3R_{365} isoform, which lacks 80 residues in the third intracellular loop (Riddy *et al.* 2016), and reduced signaling was induced by the A280V mutation in the same loop (Flores-Clemente *et al.* 2013). Further consideration to the H_3R carboxyl tail should therefore be made when assessing receptor-G protein coupling.

Ca^{2+} mobilization was detected upon exposure to the H_3R agonist RAMH in HEK-293 cells transfected with H_3R_{427}-$G\alpha_{qi4}$ (Figure 1E). Whereas this may appear to be an undesirable result, it further supports the formation of $A_{2A}R/H_3R$ heterodimers because H_3R_{427}-$G\alpha_{qi4}$ function was not observed after co-transfection with $A_{2A}Rs$, suggesting a preference of the H_3R to form hetero- over homo-dimers.

An important part of describing a new heterodimer is to find changes in the signaling profiles of the receptors involved in the dimer. In this regard, we found enhanced signaling efficacy of the agonist CGS-21680 when the H_3R was co-transfected and co-activated in the HEK293-$A_{2A}R$ cells. This effect can be explained by a H_3R-mediated facilitation of the $A_{2A}R$ coupling to G proteins, leading to an increase in the receptor efficacy to activate $G\alpha_s$ proteins and thus to produce cAMP. Given that in the absence of RAMH, CGS-21680 behaved the same in HEK293-$A_{2A}R$ cells and in HEK293-$A_{2A}R/H_3R$ cells, receptor expression does not appear to account for the observed effects.

Canonically H_3R couples to $G\alpha_{i/o}$ proteins which inhibit adenylyl cyclase activity and accordingly, activation of the receptor with RAMH lead to a decrease in cAMP formation. Similar to the observed in the calcium mobilization assays, expression of the $A_{2A}R$ changed the H_3R-mediated cAMP response from inhibition to an increase in the cAMP formation. In

the calcium assays we did not observed signaling of the H_3R through the $G\alpha_{qs4}$ proteins bound to the truncated $A_{2A}R$, and we are thus not considering a H_3R change in signaling pathways as an explanation for this effect. Therefore, we hypothesized that in the $A_{2A}R/H_3R$ heteromer the $A_{2A}R$ signaling prevails over H_3R, while the latter signaling is hampered possibly by a steric impediment. This is in line with the loss of calcium signaling when H_3R-$G\alpha_{qi4}$ was co-expressed with $A_{2A}R$.

An unexpected but interesting finding was the potential biased-signaling at the $A_{2A}R/H_3R$ heteromer, as evidenced by the incapability of the endogenous ligand histamine to signal at the $A_{2A}R/H_3R$ heteromer compared to the exogenous agonist RAMH. This discrepancy suggests that RAMH induces conformational changes in the H_3R that allow the interaction to occur, whereas the histamine-induced changes appear not sufficient for heteromerization or at least for the heteromer to signal. Ligand bias could also be explained by agonist residence time, this is, the time that a particular drug remains in its binding pocket and that will directly determine the time that a given receptor maintains an active conformation. The active state induced by histamine may therefore have a shorter duration compared with that induced by RAMH, preventing the former from activating the chimeric G proteins bound to the $A_{2A}R_{302}$. Binding studies with striatal membranes and histamine show that the first hypothesis holds better because histamine induced an increase in the affinity of the $A_{2A}R$ for its agonist CGS-21680 (Supplementary figure 4), opposite to the decrease in affinity change induced by RAMH in the same preparation. This result suggests that histamine and RAMH lock the H_3R in different conformational states that affect its interaction with the $A_{2A}R$.

4.2 Synaptic location of the $A_{2A}R/H_3R$ interaction

A previous report indicates equal distribution of $A_{2A}Rs$ in total and synaptosomal membranes from rat striatum (Rebola *et al*., 2005), with a preferential location on the post-synaptic density fraction over the pre-synaptic active zone fraction (49.2 ± 3.3 % and 26.9 ± 3.3 % of total immunoreactivity, respectively). H_3Rs are expressed pre- and post-synaptically (Ellenbroek and Ghiabi, 2014), but they seem to be highly enriched in the terminals of striato-pallidal neurons (iMSNs) yielding a value of 1,327 ± 79 fmol/mg protein (Morales-Figueroa e*t al*., 2014). Given this distribution, our results point to a specific synaptic location of the $A_{2A}R/H_3R$ heteromer that provides the interaction a preferential role in pre-synaptic modulation of glutamatergic or GABAergic transmission.

In the striatum, $A_{2A}Rs$ have a specific location in iMSNs (Schiffman *et al*., 1991) and cortico-dMSNs terminals, but not in the cortico-iMSNs projections (Quiróz *et al*., 2009). It has also been reported that the $A_{2A}R$ antagonists KW-6002 and SCH-442416 can differentiate either $A_{2A}R$ location, respectively (Orrú *et al*., 2011). Although there are no agonists capable to differentiate between $A_{2A}R$ populations, this information may be a valuable tool for targeting and modulating the $A_{2A}R$ and H_3R pharmacology in a location-specific manner, using bivalent ligands directed to the heterodimer. Speculating on the potential therapeutic role of the $A_{2A}R/H_3R$ -heteromer and assuming an increase in the $A_{2A}R$ signaling, targeting the cortico-striatal heteromer may have relevance for the treatment of attention deficit and hyperactivity disorder, autism and obsessive and compulsive disorder by modulating the dimer signaling to dMSNs.

5. Conclusion

This study presents for the first time evidence for an $A_{2A}R/H_3R$ heterodimer based on functional complementation and co-immunoprecipitation assays in HEK-293 cells, where co-activation of the receptors leads to enhanced $A_{2A}R$ signaling and attenuation of H_3R functionality. In rat striatal tissue the interaction occurs in synapses where H_3R activation modifies the binding affinity of the $A_{2A}R$.

Acknowledgements

We thank Juan Escamilla-Sánchez and Raúl González-Pantoja for excellent technical assistance. R. M.-G. held a Conacyt graduate scholarship (244993).

Author contributions

R. M.-G., R. v. R. and J.-A. A.-M. designed the study; R. M.-G., C. G.-R., J.-M. A. and M. T. R. performed the experiments; R. M.-G., J.-A. O.-R., R. v. R. and J.-A. A.-M. performed data analysis. R. M.-G., R. v. R. and J.-A. A.-M. wrote the manuscript. All authors revised and approved the manuscript.

Conflicts of interest

The authors disclose no conflict of interest.

Funding

This work was supported by Cinvestav, Conacyt (grant 220448 to J.-A. A.-M.), PAPIIT-UNAM (grant IN216215 to J.-M. A.), the National Institute on Alcohol Abuse and Alcoholism (grant AA20539 to R. M. v R.) and the Ralph W. and Grace M. Showalter Research Trust (to R. M. v R.). The funding sources were not involved at all in the study design, collection, analysis and interpretation of data, writing of the manuscript or the decision to submit this report.

6. References

Arias-Montaño J.A., Floran B., Garcia M., Aceves J., Young J.M., 2001. Histamine H_3 receptor-mediated inhibition of depolarization-induced, dopamine D_1 receptor-dependent release of [^{3}H]-gamma-aminobutyric acid from rat striatal slices. Br J Pharmacol 133:165-171

Berjukow S., Döring F., Froschmayr M., Grabner M., Glossmann H., Hering S., 1996. Endogenous calcium channels in human embryonic kidney (HEK293) cells. Br J Pharmacol 118:748-754

Bolam J.P., Hanley J.J., Booth P.A., Bevan M.D., 2000. Synaptic organization of the basal ganglia. J Anat 196:527-542

Bolam P.J., Ellender T.J., 2016. Histamine and the striatum. Neuropharmacology 106:74-84

Cabello N., Gandía J., Bertarelli D.C.G., Watanabe M., Lluís C., Franco R., Ferré S., Luján R., Ciruela F., 2009. Metabotropic glutamate type 5, dopamine D_2 and adenosine A_{2a} receptors from higher-order oligomers in living cells. J Neurochem 109:1497-1507

Carriba P., Ortiz O., Patkar K., Justinova Z., Stroik J., Themann A., Muller C., Woods AS., Hope BT., Ciruela F., Casadó V., Canela E.I., Lluis C., Goldberg S.R., Moratalla R., Franco R., Ferré S., 2007. Striatal adenosine A_{2A} and cannabinoid CB_1 receptors form functional heteromeric complexes that mediate the motor effects of cannabinoids. Neuropsycopharmacology 32:2249-2259

Chiang T., Sansuk K., van Rijn R.M., 2016. β-arrestin 2 dependence of δ opioid receptor agonists is correlated with alcohol intake. Br J Pharmacol 173:332-343

Ciruela F., Casadó V., Rodrigues R.J., Luján R., Burgueño J., Canals M., Borycz J., Rebola N., Goldberg S.R., Mallol J., Cortés A., Canela E.I., López-Giménez J.F., Milligan G., Lluis C., Cunha R.A., Ferré S., Franco R., 2006. Presynaptic control of striatal glutamatergic neurotransmission by adenosine A_1-A_{2A} receptor heteromers. J Neurosci 26:2080-2087

Cogé F., Guénin S.P., Audinot V., Renouard-Try A, Beauverger P, Macia C, Ouvry C, Nagel N, Rique H, Boutin JA, Galizzi JP., 2001. Genomic organization and characterization of splice variants of the human histamine H_3 receptor. Biochem J 355:279-288

Conklin BR, Herzmark P, Ishida S, Voyno-Yasenetskaya TA, Sun Y, Farfel Z, Bourne HR., 1996. Carboxyl terminal mutations of Gq alpha and Gs alpha that alter the fidelity of receptor activation. Mol Pharmacol 50:885-890

Doreulee N, Yanovsky Y, Flagmeyer I, StevensDR, Haas HL, Brown RE., 2001. Histamine H_3 receptors depress synaptic transmission in the corticostriatal pathway. Neuropharmacology 40:106-113

Ellenbroek BA., 2013. Histamine H_3 receptors, the complex interaction with dopamine and its implications for addiction. Br J Pharmacol 170:46-57

Ellenbroek B.A., Ghiabi B., 2014. The other side of the histamine H_3 receptor. Trends Neurosci 37:191-199

Ferré S., Ciruela F., Canals M., Marcellino D., Burqueno J., Casadó V., Hillion J., Torvinen M., Fanelli F., Benedetti P.D., Goldberg S.R., Bouvier M., Fuxe K., Agnati L.F., Lluis C., Franco R., Woods A., 2004. Adenosine A_{2A}-dopamine D_2 receptor-receptor heteromers. Targets for neuro-psychiatric disorders Parkinsonism. Relat Disord 10:265-271

Ferré S., Fredholm B.B., Moreli M., Popoli P., Fuxe K., 1997. Adenosine-dopamine receptor-receptor interactions as an integrative mechanism in the basal ganglia. Trends Neurosci 20:482-487

Flores-Clemente C., Osorio-Espinoza A., Escamilla-Sánchez J., Leurs R., Arias J.M., Arias-Montaño J.A., 2013. A single-point mutation (Ala280Val) in the third intracellular loop alters the signaling properties of the human histamine H_3 receptor stably expressed in CHO-K1 cells. Br J Pharmacol 170:127-135

Gonzalez-Sepulveda M., Rosell S., Hoffman H.M., Castillo-Ruíz Ma. del Mar., Mignon V., Moreno-Delgado D., Vignes M., Diaz J., Sabria J., Ortiz J., 2013. Cellular distribution of the histamine H_3 receptor in the basal ganglia: Functional modulation of dopamine and glutamate neurotransmission. Basal Ganglia 3:109-121

Gubitz A.K., Widdowson L., Kurokawa M., Kirkpatrick K.A., Richardson P.J., 1996. Dual signaling by the adenosine A_{2a} receptor involves activation of both N- and P-type calcium channels by different G proteins and protein kinases in the same striatal nerve terminals. J Neurochem 67:374-381

Han Y., Moreira I.S., Urizar E., Weinstein H., Javitch J.A., 2009. Allosteric communication between protomers of dopamine class A GPCR dimers modulates activation. Nat Chem Biol 5:688-695

Hillion J., Canals M., Torvinen M., Casado V., Scott R., Terasmaa A., Hansson A., Watson S., Olah M.E., Canela E.I., Zoli M., Agnati L.F., Ibanez C.F., Lluis C., Franco R., Ferre S., Fuxe K., 2002. Coaggregation, cointernalization, and codesensitization of adenosine A_{2A} receptors and dopamine D_2 receptors. J Biol Chem 277:18091-18097

Kemp J.M., Powell T.P., 1971. The structure of caudate nucleus of the cat: light and electron microscopy. Philos Trans R Sot Lond B Biol Sci 262:383-401.

Kirk I.P. and Richardson P.J., 1994. Adenosine A_{2a} receptor-mediated modulation of striatal [^{3}H]GABA and [^{3}H]acetylcholine release. J Neurochem 62:960-966

Kirk I.P., Richardson P.J., 1995. Inhibition of striatal GABA release by the adenosine A_{2A} receptor is not mediated by increase in cyclic AMP. J Neurochem 64:2801-2808

Márquez-Gómez, R., Gutierrez-Rodelo, C., Robins, M. T., Escamilla-Sánchez, J., Olivares-Reyes, J.-A., van Rijn, R., Arias-Montaño, J.-A., 2016. On the existence of a histamine H_3–adenosine A_{2A} receptor heteromer. Inflamm Res 65 (Suppl. 1), S29

Morales-Figueroa G.E., Márquez-Gómez R., González-Pantoja R., Escamilla-Sanchez J., Arias-Montaño J.A., 2015. Histamine H_3 receptor activation counteracts adenosine A_{2A} receptor-mediated enhancement of depolarization-evoked [^{3}H]-GABA release from rat globus pallidus synaptosomes. ACS Chem Neurosci 20:637-645

Moreno E., Moreno-Delgado D., Navarro G., Hoffmann H.M., Fuentes S., Rosell-Vilar S., Gasperini P., Rodriguez-Ruiz M., Medrano M., Mallol J., Cortés A., Casadó V., Lluis C., Ferré S., Ortiz J., Canela E., McCormick P.J., 2014. Cocaine disrupts histamine H_3 receptor modulation of dopamine D_1 receptor signaling: σ_1-D_1-H_3 receptor complexes as key targets for reducing cocaine's effects. J Neurosci 34:3545-3558

Nieto-Alamilla G., Márquez-Gómez R., García-Gálvez A.-M., Morales-Figueroa G.-E., Arias-Montaño J.-A., 2016. The Histamine H_3 Receptor: Structure, Pharmacology and Function. Mol Pharmacol 90:649-673

Panula P., Nuutinen S., 2013. The histaminergic network in the brain: basic organization and role in disease. Nat Rev Neurosci 14:472-487

Passani M.B., Blandina P., 2011. Histamine receptors in the CNS as target for therapeutic intervention. Trends Pharmacol Sci 32:242-249

Pillot C., Heron A., Cochois V., Tardivel-Lacombe J., Ligneau X., Schwartz J.-C., Arrang J.-M., 2002. A detailed mapping of the histamine H_3 receptor and its gene transcripts in rat brain. Neuroscience 114:173-193

Popoli P., Betto P., Reggio R., Ricciarello G., 1995. Adensoine A_{2A} receptor stimulation enhances strital extracellular glutamate levels in rats. Eur J Pharmacol 287:215-217

Prast H., Tran M.H., Fischer H., Kraus M., Lamberti C., Grass K., Philippu A., 1999. Histaminergic neurons modulate acetylcholine release in the ventral striatum: role of H_3 histamine receptors. Naunyn Schmiedebergs Arch Pharmacol 360:558-564

Quiroz C., Luján R., Chigashima M., Simoes A.P., Lerner T.N., Borycz J., Kachroo A., Canas P.M., Orru M., Schwarzschild M.A., Rosin D.L., Kreitzer A.C., Cunha R.A., Watanabe M., Ferré S., 2009. Key modulatory role of presynaptic adenosine A_{2A} receptors in cortical neurotransmission to the striatal direct pathway. Scientific World Journal 18:1321-1344

Riddy D.M., Cook A.E., Diepenhorst N.A., Bosnyak S., Brady R., Mannoury la Cour C., Mocaer E., Summers R.J., Charman W.N., Sexton P.M., Christopoulos A., Langmead C.J., 2016. Isoform-specific biased agonism of histamine H_3 receptor agonists. Mol Pharmacol 91:87-99

Rivera-Ramírez N., Montejo-López W., López-Méndez M.C., Guerrero-Hernández A., Molina-Hernández A., García-Hernández U., Arias-Montaño J.A., 2016. Histamine H3 receptor activation stimulates calcium mobilization in a subpopulation of rat striatal neurons in primary culture, but not in synaptosomes. Neurochem Int 101:38-47

Rodríguez-Ruiz M., Moreno E., Moreno-Delgado D., Navarro G., Mallol J., Cortés A., Lluís C., Canela E.I., Casadó V., McCormick P.J., Franco R., 2016. Heteroreceptor complexes formed by dopamine D_1, histamine H_3, and N-Methyl-D-Aspartate glutamate receptors as targets to prevent neuronal death in Alzheimer´s disease. Mol Neurobiol. (in press) doi:10.1007/s12035-016-9995-y

Schiffmann S.N., Jacobs O., Vanderhaeghen J.J., 1991. Striatal restriacted adenosine A_2 receptor (RDC8) is expressed by enkephalin but not by subtance P neurons: an in situ hybridization histochemestry study. J Neurochem 57:1062-1067

Schliker E., Fink K., Detzner M., Gothert M., 1993. Histamine inhibits dopamine release in the mouse striatum via presynaptic H_3 receptors. J Neural Transm Gen Sect 93:1-10

Schwarzschild M.A., Agnati L., Fuxe K., Chen J.F., Morelli M., 2006. Targeting adenosine A_{2A} receptor in Parkinson´s disease. Trends Neurosci 29:647-654

Tapper J.M., Kóos T., Wilson C.J., 2004. GABAergic microcircuits in the neoestriatum. Trends Neurosci 27:662-669.

Thomas P., Smart T.G., 2005. HEK293 cells line: A vehicle for the expression of recombinant proteins. J Pharmacol and Toxicol Methods 51:187-200

van Rijn R.M., Harvey J.H., Brissett D.I., DeFriel J.N., Whistler J.L., 2013. Novel screening assay for the selective detection of G-protein-coupled receptor heteromer signaling. J Pharmacol Exp Ther 344:179-188

Legends for Figures

Figure 1. Adenosine A_{2A} and histamine H_3 receptors co-immunoprecipitate in transfected HEK-293 cells. A. Co-immunoprecipitation of the hemagglutinin-tagged H_3R (3xHA-H_3R) with the $A_{2A}R$ in protein extracts from HEK-293 cells. A 45 kDa band corresponding to the $A_{2A}R$ was detected. This band was not observed with the negative control. Input corresponds to 30% of the total protein. An antibody against the D_2 receptor (α-D_2R) was used as a negative control. Blots are representative of 3 independent experiments.

Figure 2. Study of the possible $A_{2A}R/H_3R$ dimerization by functional complementation assay. A. Basis of the assay. The G protein-coupled receptor (GPCR; grey cylinders) is truncated at its carboxyl terminus to generate a nonfunctional GPCR, which is then fused to the chimeric G protein (green hexagons). The chimeric G protein is formed by a $G\alpha_q$ protein in which 9 or 10 residues of the C-terminus were substituted by the corresponding sequence of a $G\alpha_{s4}$ or $G\alpha_{i4}$ protein (represented by X). Under these conditions, Ca^{2+} mobilization can only be elicited when the complex GPCR-$G\alpha_{qx}$ is in close proximity to a wild type (WT) GPCR, either the same (homodimerization) or a different receptor (heterodimerization). B. Activation of the H_3R with its agonist RAMH resulted in Ca^{2+} mobilization only when it was co-expressed with the chimeric $G\alpha_{qi4}$ but not when transfected alone. C. When activated with its agonist CGS-21680, the $A_{2A}R$ was uncapable to induce Ca^{2+} mobilization either alone or when co-transfected with the chimeric $G\alpha_{qs4}$ protein. D. Functional complementation by homodimerization of the truncated $A_{2A}R_{302}$, either bound to $G\alpha_{qs4}$ ($A_{2A}R_{302}$-$G\alpha_{qs4}$) or $G\alpha_{qi4}$ ($A_{2A}R_{302}$-$G\alpha_{qi4}$), with the native $A_{2A}R$ was not observed. E. Activation of the truncated H_3R_{427} bound to $G\alpha_{qi4}$ (H_3R_{427}-$G\alpha_{qi4}$) induced

Ca^{2+} mobilization on its own and homodimerization with the WT-H_3R did not modify the response. No signal was observed with activation of the H_3R_{427}-$G\alpha_{qs4}$ construct when it was co-expressed with the WT-H_3R. In all graphs data are means ± SEM from 3 replicates from a representative experiment. The quantitative analysis is shown in Table 1 and 4.

Figure 3. Ligand modulation of the $A_{2A}R/H_3R$ interaction in HEK-293 cells. Activation of the WT-H_3R with its agonist RAMH led to functional complementation when co-expressed with the $A_{2A}R_{302}$-$G\alpha_{qi4}$ but not with $A_{2A}R_{302}$-$G\alpha_{qs4}$. B. Ca^{2+} mobilization was not observed when the WT-$A_{2A}R$ was co-transfected with the truncated H_3R_{427}-$G\alpha_{qs4}$ or H_3R_{427}-$G\alpha_{qi4}$, in accord with the incapability of the receptor to activate the chimeric proteins. C. As shown in Figure 1D, activation of the H_3R_{427}-$G\alpha_{qi4}$ resulted in Ca^{2+} mobilization, and this response was prevented when it was co-expressed with the WT-$A_{2A}R$, suggesting a preference of the H_3R_{427}-$G\alpha_{qi4}$ to form heterodimers. D. The well-studied $A_{2A}R/D_2R$ heterodimer was used as a positive control for these experiments. Activation of the D_2R with increasing concentrations of the agonist quinpirole caused marked Ca^{2+} mobilization only when co-expressed with the chimeric $A_{2A}R_{302}$-$G\alpha_{qi4}$. E. H_4R as a negative control. No functional complementation was observed when the receptor was co-expressed with the $A_{2A}R_{302}$-$G\alpha_{qi4}$, showing the specificity of the $A_{2A}R/H_3R$ interaction. F. Functional complementation between the $A_{2A}R_{302}$-$G\alpha_{qi4}$ and the WT-H_3R was not observed when the latter receptor was activated with the endogenous agonist histamine. For all graphs data are means ± SEM from 3 replicates from representative experiments. The quantitative analysis is shown in Table 1.

Figure 4. H_3R activation enhances $A_{2A}R$-mediated cAMP signaling in HEK-293 cells. A. Activation of the $G\alpha_s$-coupled $A_{2A}R$ with its agonist CGS-21680 induced cAMP formation and H_3R co-activation enhanced $A_{2A}R$ efficacy. Co-expression of the H_3R did not modified the $A_{2A}R$ functional response. Values for pEC_{50} and maximal effect (Emax) are given in Table 2. B. H_3R activation with RAMH decreased forskolin-induced cAMP formation in accord with the inhibitory nature of the $G\alpha_{i/o}$-coupled receptor. $A_{2A}R$ expression and receptors co-activation lead to a change in the H_3R signaling. Data are means ± SEM from 3-5 independent experiments. Values for pIC_{50} and maximal effect (Imax) are given in Table 2.

Figure 5. H_3R activation decreases $A_{2A}R$ affinity for the agonist CGS-21680 in synaptosomal membranes but not in membranes from the whole striatum. A. The H_3R co-immunoprecipitated with the $A_{2A}R$ in a protein extract of Percoll-purified striatal synaptosomes. The band of ~45 KDa corresponds to the expected migration of the H_3R. No band was observed in the negative control (αCD81). B. Co-immunoprecipitation of the $A_{2A}R$ with the H_3R in a protein extract of striatal synaptosomes. A band of ~45 KDa corresponds to the expected migration of the H_3R.The figure depicts representative blots, repeated a further 4 times with similar results. C. CGS-21680 (10 and 100 nM) did not modify the H_3R affinity for its ligand [^{3}H]-NAMH in membranes isolated from striatal synaptosomes. D. In the same preparation, the H_3R agonist RAMH (100 nM) decreased the $A_{2A}R$ affinity for [^{3}H]-CGS-21680. Values are means ± SEM from 3 replicates from a representative experiment. E. Analysis of 3 independent experiments. The statistical analysis was performed with paired Student's *t* test. F. H_3R activation with RAMH (100 nM) failed to decreased the $A_{2A}R$ affinity for [^{3}H]-CGS-21680 in membranes from the

whole striatum. Values are means ± SEM from 3 replicates from a representative experiment.

Legends for Supplementary Figures

Supplementary Figure 1. A. The activation of the $G\alpha_s$-coupled histamine H_2 receptor did not induce Ca^{2+} mobilization wen transfected alone, but did so when the $G\alpha_{qs}$ was co-expressed, proving the functionality of the chimeric protein. B. The truncated H_3Rs of 421 and 411 residues were unable to induce Ca^{2+} mobilization and functional complementation was not observed by homodimerization with either receptor. C. Functional complementation assay showing that the co-activation of the WT-H_3R with increasing concentrations of RAMH and the $A_{2A}R_{302}$-$G\alpha_{qs}$ with a fixed concentration of CGS-21680 did not modified the response. D. The co-activation of the H_3R_{427}-$G\alpha_{qi4}$ and the WT-A_{2A}R did not recover the Ca^{2+} response observed when the second construct was transfected alone.

Supplementary Figure 2. Effect of histamine and RAMH on the H_3R and H_4R and cAMP modulation of the $A_{2A}R/H_3R$ heterodimer A. Histamine induced Ca^{2+} mobilization by activation of the H_3R only when the $G\alpha_{qi4}$ was expressed. B. Activation of the H_4R with histamine caused a Ca^{2+} response promoted by the $G\alpha_{qi4}$. No response was observed by the solely transfection of the H_4R. C and D. Plots showing the cAMP formation experiments expressed as percentage of the basal. C. A_{2A}R signaling is increased after co-activation with the H_3R. No change in the CGS-21680 efficacy or potency was observed when H_3R was co-expressed with A_{2A}R. D. A_{2A}R co-expression and co-activation caused a prevention of H_3R-medited cAMP inhibition, suggesting the prevalence of A_{2A}R signaling in the heterodimer. The means ± SEM are shown in table 2.

Supplementary Figure 3. Transmission electron microscopy of rat striatal synaptosomes. A. Abundant presence of isolated terminals (arrow heads). Other common components such as mitochondrion (m) and myelin fragments (M) can be observed. B. Close view of a pre-synaptic terminal, distinguishable by the synaptic vesicles (v) and mitochondria, making contact with a post-synaptic element (p). The pre-synaptic active zone and the post-synaptic density can be distinguished.

Supplementary Figure 4. Effect of the endogenous H_3R agonist histamine on the $A_{2A}R$ affinity for its agonist [^{3}H]CGS-21680. A. Histamine (1 μM) increased $A_{2A}R$ affinity for CGS-21680. Values are means ± SEM from 5 replicates from a representative experiment. B. Analysis of 4 independent experiments. The statistical analysis was performed with paired Student's *t* test.

Table 1. Pharmacological characteristics of the $A_{2A}R/H_3R$ functional complementation assays in transfected HEK-293 cells

Transfection	Agonist	Emax (%)	pEC_{50}
$H_3R + G\alpha_{qi4}$	RAMH	419 ± 25	7.73 ± 0.31
	Histamine	504 ± 22[b]	6.19 ± 0.17[b]
H_3R_{427}-$G\alpha_{qi4}$	RAMH	753 ± 41	7.14 ± 0.21
H_3R_{427}-$G\alpha_{qi4}$ + H_3R	RAMH	523 ± 41[b]	7.38 ± 0.34
$A_{2A}R_{302}$-$G\alpha_{qi4}$ + H_3R	RAMH	449 ± 25	7.31 ± 0.23
	RAMH + CGS	429 ± 14[n.s.]	7.63 ± 0.15
$H_4R + G\alpha_{qi4}$	Histamine	725 ± 51	6.35 ± 0.25
	RAMH	551 ± 27[a]	6.15 ± 0.16
$H_2R + G\alpha_{qs4}$	Dimaprit	860 ± 37	6.15 ± 0.12
$A_{2A}R_{302}$-$G\alpha_{qi4}$ + D_2R	Quinpirole	612 ± 34	6.47 ± 0.22

Data are means ± SEM from 3 experiments. Statistical comparisons were performed between two agonists for the same transfection, or between the transfection with the chimeric receptor and the transfection of the chimeric receptor plus the wild type receptor. [a] $P < 0.05$; [b] $P < 0.01$, Student's *t* test. Both RAMH and CGS-21680 were assayed at 100 nM. RAMH, R-α-methylhistamine; CGS, CGS-21680.

Table 2. Pharmacological characteristics of the cyclic AMP (cAMP) formation assay in transfected HEK-293 cells.

Transfection	Agonist	pEC_{50}	Emax (%)	pIC_{50}	Imax (%)
$A_{2A}R$	CGS	8.0 ± 0.4	152 ± 7	-	-
$A_{2A}R + H_3R$	CGS	8.7 ± 0.5	153 ± 7	-	-
$A_{2A}R + H_3R$	+RAMH	8.0 ± 0.2	248 ± 9[b]	-	-
H_3R	RAMH	-	-	8.1 ± 0.3	-26 ± 2
$H_3R + A_{2A}R$	RAMH	10.6 ± 1	114 ± 3	-	-
$H_3R + A_{2A}R$	+CGS	9.9 ± 0.6	120 ± 2	-	-

Data are means ± SEM from 3-5 experiments. Comparison was performed between the solely transfection of a receptor vs co-transfection of both receptors. N.D., not determined. [a] $P < 0.05$; [b] $P < 0.01$. Student's *t* test. Both RAMH and CGS-21680 were tested at 100 nM. RAMH, R-α-methylhistamine; CGS, CGS-21680; FSK, Forskolin.

Table 3. Analysis of binding assays in rat striatal membranes

	pKi	Bmax (%)
[^{3}H]-NAMH		
Synaptosomes		
RAMH	9.09 ± 0.22	100.0 ± 0.3
RAMH + CGS 10 nM	8.99 ± 0.02^{ns}	110.0 ± 4.0^{ns}
RAMH + CGS 100 nM	9.08 ± 0.06^{ns}	103.0 ± 4.1^{ns}
[^{3}H]CGS-21680		
Whole striatum		
CGS	8.06 ± 0.15	100.0 ± 14
CGS + RAMH	8.11 ± 0.04^{ns}	88.0 ± 6.0^{ns}
Synaptosomes		
CGS	8.10 ± 0.04	100.0 ± 9.0
CGS + RAMH	7.70 ± 0.04^{a}	88.1 ± 10.0^{ns}

Data are means ± SEM from 3-5 experiments. For [^{3}H]-NAMH binding assays the statistical analysis was performed with one-way Anova and Dunnett´s *post hoc* test. For [^{3}H]-CGS-21680 binding, values in the presence of RAMH were compared with the corresponding control with Student's *t* test. ^{a} $P < 0.001$, ns, not significant. CGS, CGS-21680. RAMH (R-α-methylhistamine) was tested at 100 nM in all the experiments.

Supplementary Table 1: Primers employed in the generation of the truncated A_{2A} and H_3 receptors

Fwd_3xHA + HindIII	5'-AAAAAGCTTATGTACCCATACGATGTTCC-3
Rev_3xHA-A_{2A}R-302 + BamHI	5'-AAAGGATCCGATCTTGCGGAAGG-3'
Rev_3xHA-H_3R-427 + BamHI	5'-AAAGGATCCCAGCAGCTTGGTG-3'
Rev_3xHA-H_3R-411 + BamHI	5'-AAGGATCCAGGGTAGAGGACAGGGTTGAC-3'
Rev_3xHA-H_3R-421 + BamHI	5'-AAAGGATCCCCGGCGGAAGCTGTGGTG-3'

Supplementary Table 2. Pharmacological data of all the functional complementation assays performed.

Transfection	Agonist	Emax (%)	pEC_{50}	EC_{50} (nM)
H_3R	RAMH	ND	ND	ND
	Histamine	ND	ND	ND
H_3R + $G\alpha_{qi4}$	RAMH	419 ± 25	7.73 ± 0.31	19.95
	Histamine	504 ± 22	6.19 ± 0.17	645.65
$A_{2A}R$	CGS	ND	ND	ND
$A_{2A}R$ + $G\alpha_{qs4}$	CGS	ND	ND	ND
$A_{2A}R_{302}$-$G\alpha_{qi4}$	CGS	ND	ND	ND
$A_{2A}R_{302}$-$G\alpha_{qs4}$	CGS	ND	ND	ND
$A_{2A}R_{302}$-$G\alpha_{qi4}$ + $A_{2A}R$	CGS	ND	ND	ND
$A_{2A}R_{302}$-$G\alpha_{qs4}$ + $A_{2A}R$	CGS	ND	ND	ND
H_3R_{427}-$G\alpha_{qi4}$	RAMH	753 ± 41	7.14 ± 0.21	72.44
H_3R_{427}-$G\alpha_{qs4}$	RAMH	ND	ND	ND
H_3R_{427}-$G\alpha_{qi4}$ + H_3R	RAMH	523 ± 41	7.38 ± 0.34	41.68
H_3R_{427}-$G\alpha_{qs4}$ + H_3R	RAMH	ND	ND	ND
H_3R_{411}-$G\alpha_{qi4}$	RAMH	ND	ND	ND
H_3R_{421}-$G\alpha_{qi4}$	RAMH	ND	ND	ND
H_3R_{421}-$G\alpha_{qi4}$ + H_3R	RAMH	ND	ND	ND
H_{411}-$G\alpha_{qi4}$ + H_3R	RAMH	ND	ND	ND

$A_{2A}R_{302}$-$G\alpha_{qi4}$ + H_3R	RAMH	449 ± 25	7.31 ± 0.23	48.97
	CGS	429 ± 14	7.63 ± 0.15	23.44
	+ RAMH			
$A_{2A}R$-$G\alpha_{qs4}$ + H_3R	RAMH	ND	ND	ND
H_3R_{427}-$G\alpha_{qs4}$ + $A_{2A}R$	CGS	ND	ND	ND
H_3R_{427}-$G\alpha_{qi4}$ + $A_{2A}R$	CGS	ND	ND	ND
	CGS	ND	ND	ND
	+ RAMH			
H_4R	Histamine	ND	ND	ND
	RAMH	ND	ND	ND
H_4R + $G\alpha_{qi4}$	Histamine	725 ± 51	6.35 ± 0.25	446.68
	RAMH	551 ± 27	6.15 ± 0.16	794.32
$A_{2A}R_{302}$-$G\alpha_{qi4}$ + H_3R	Histamine	ND	ND	ND
$A_{2A}R_{302}$-$G\alpha_{qi4}$ + H_4R	Histamine	ND	ND	ND
$A_{2A}R_{302}$-$G\alpha_{qi4}$ + D_2R	Quinpirole	612 ± 34	6.47 ± 0.22	338.84
D_2R	Quinpirole	ND	ND	ND
H_2R + $G\alpha_{qs4}$	Dimaprit	860 ± 37	6.15 ± 0.12	707.94
H_2R	Dimaprit	ND	ND	ND

Data are means ± SEM from 3 experiments. RAMH and CGS-21680 were tested at 100 nM. RAMH: R-α-methylhistamine; CGS: CGS-21680. ND; not determined.

Figure 1

A

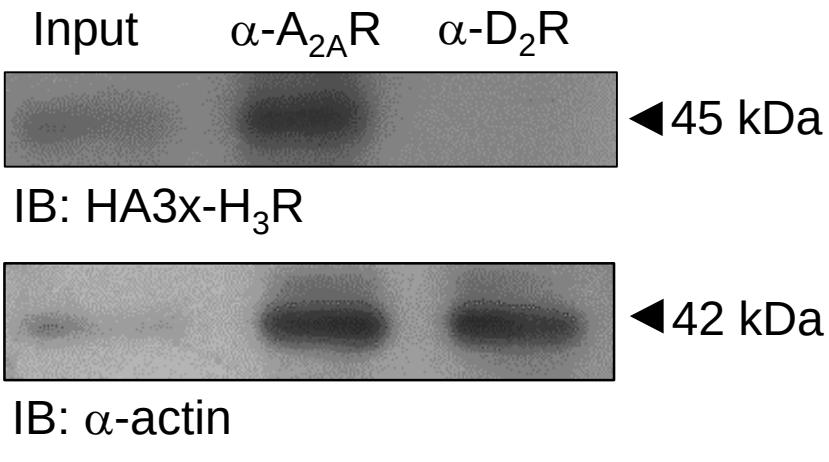

Figure 2

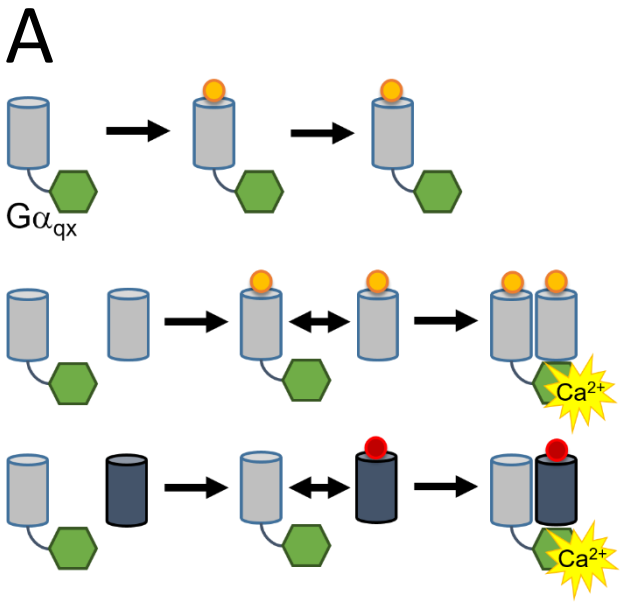
A
Gαqx
Ca2+
Ca2+

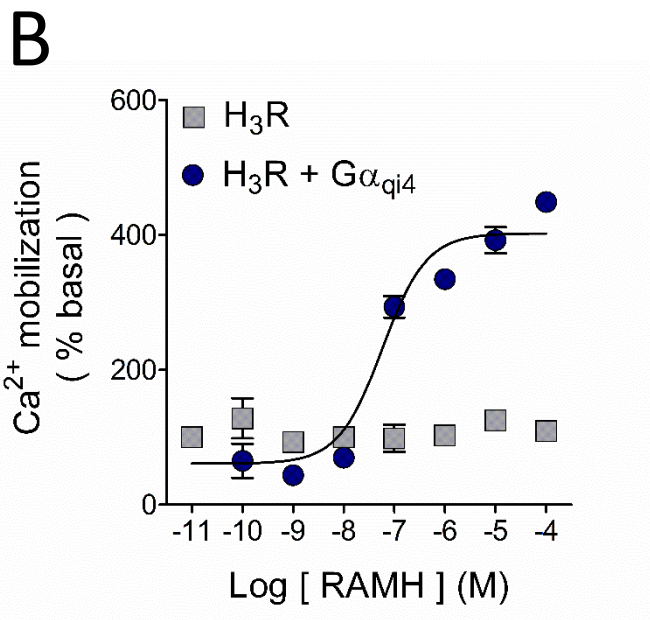
B
H3R
H3R + Gαqi4
Ca2+ mobilization (% basal)
600
400
200
0
-11 -10 -9 -8 -7 -6 -5 -4
Log [RAMH] (M)

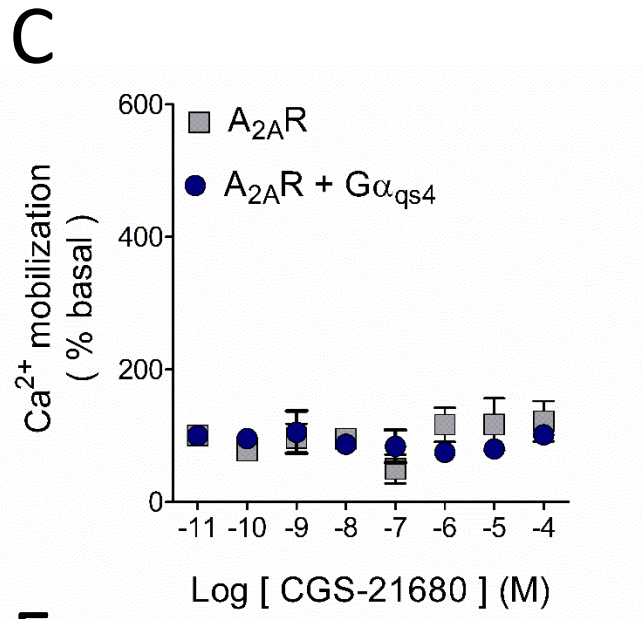
C
A2AR
A2AR + Gαqs4
Ca2+ mobilization (% basal)
600
400
200
0
-11 -10 -9 -8 -7 -6 -5 -4
Log [CGS-21680] (M)

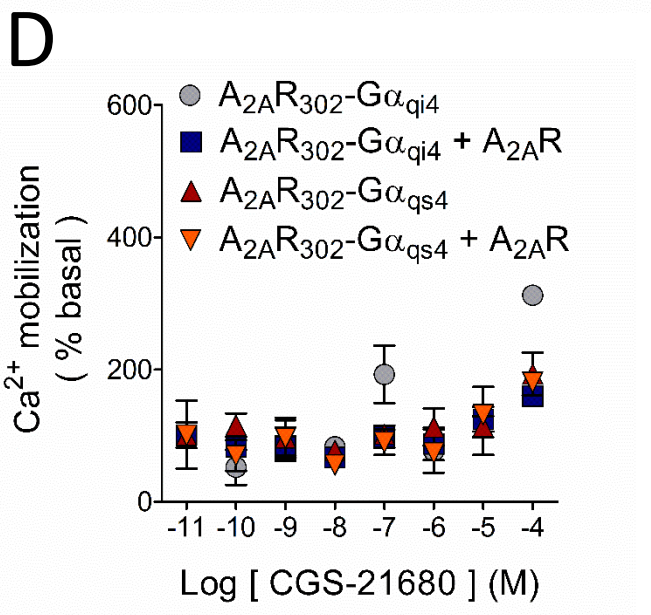
D
A2AR302-Gαqi4
A2AR302-Gαqi4 + A2AR
A2AR302-Gαqs4
A2AR302-Gαqs4 + A2AR
Ca2+ mobilization (% basal)
600
400
200
0
-11 -10 -9 -8 -7 -6 -5 -4
Log [CGS-21680] (M)

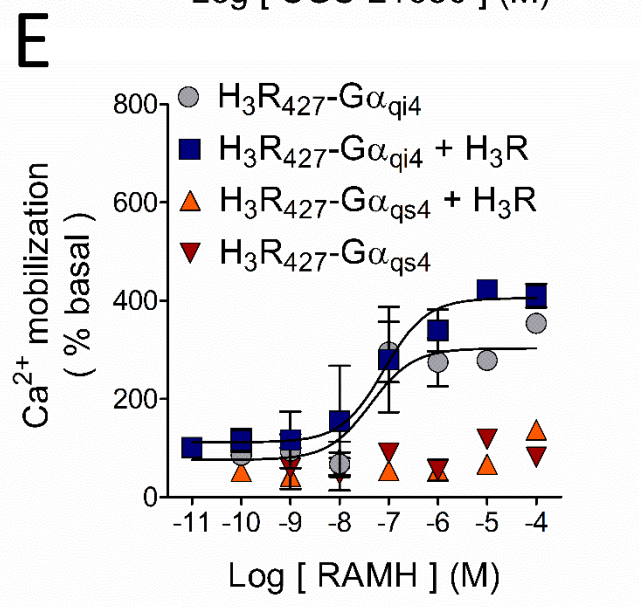
E
H3R427-Gαqi4
H3R427-Gαqi4 + H3R
H3R427-Gαqs4 + H3R
H3R427-Gαqs4
Ca2+ mobilization (% basal)
800
600
400
200
0
-11 -10 -9 -8 -7 -6 -5 -4
Log [RAMH] (M)

Figure 3

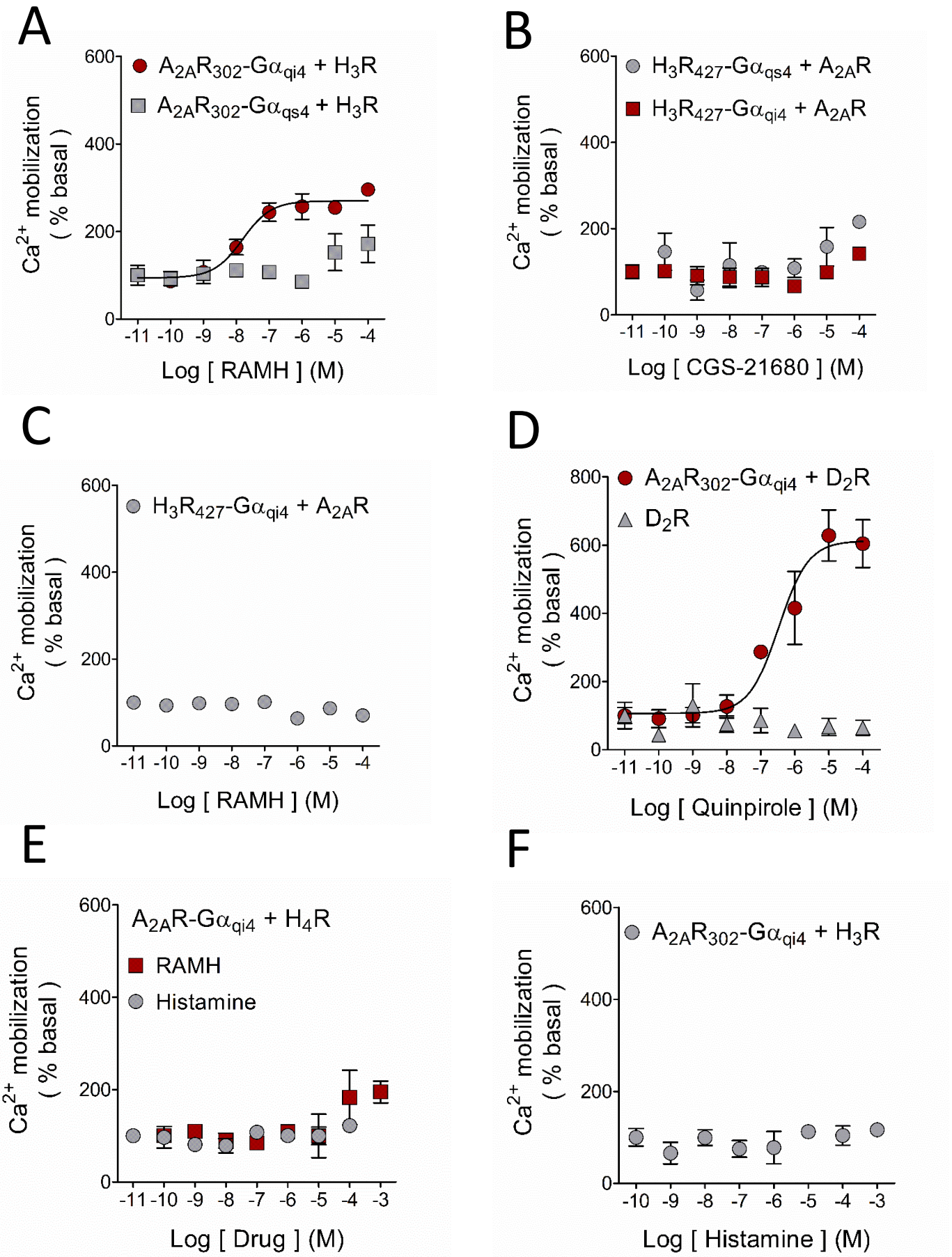
A
B
C
D
E
F
$A_{2A}R_{302}$-$G\alpha_{qi4}$ + H_3R
$A_{2A}R_{302}$-$G\alpha_{qs4}$ + H_3R
H_3R_{427}-$G\alpha_{qs4}$ + $A_{2A}R$
H_3R_{427}-$G\alpha_{qi4}$ + $A_{2A}R$
$A_{2A}R_{302}$-$G\alpha_{qi4}$ + D_2R
D_2R
$A_{2A}R$-$G\alpha_{qi4}$ + H_4R
RAMH
Histamine
Ca^{2+} mobilization (% basal)
Log [RAMH] (M)
Log [CGS-21680] (M)
Log [Quinpirole] (M)
Log [Drug] (M)
Log [Histamine] (M)

Figure 4

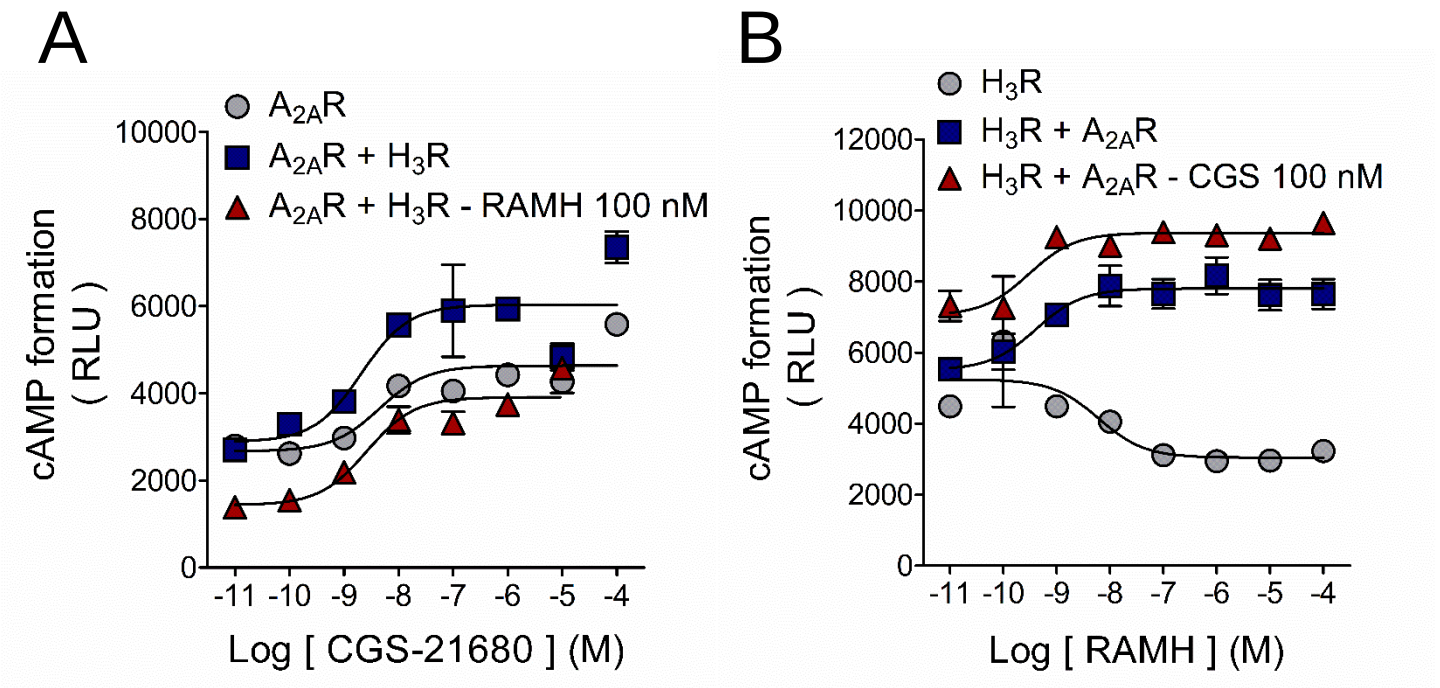
A
$A_{2A}R$
$A_{2A}R + H_3R$
$A_{2A}R + H_3R$ - RAMH 100 nM
cAMP formation (RLU)
10000
8000
6000
4000
2000
0
-11 -10 -9 -8 -7 -6 -5 -4
Log [CGS-21680] (M)
B
H_3R
$H_3R + A_{2A}R$
$H_3R + A_{2A}R$ - CGS 100 nM
cAMP formation (RLU)
12000
10000
8000
6000
4000
2000
0
-11 -10 -9 -8 -7 -6 -5 -4
Log [RAMH] (M)

Figure 5

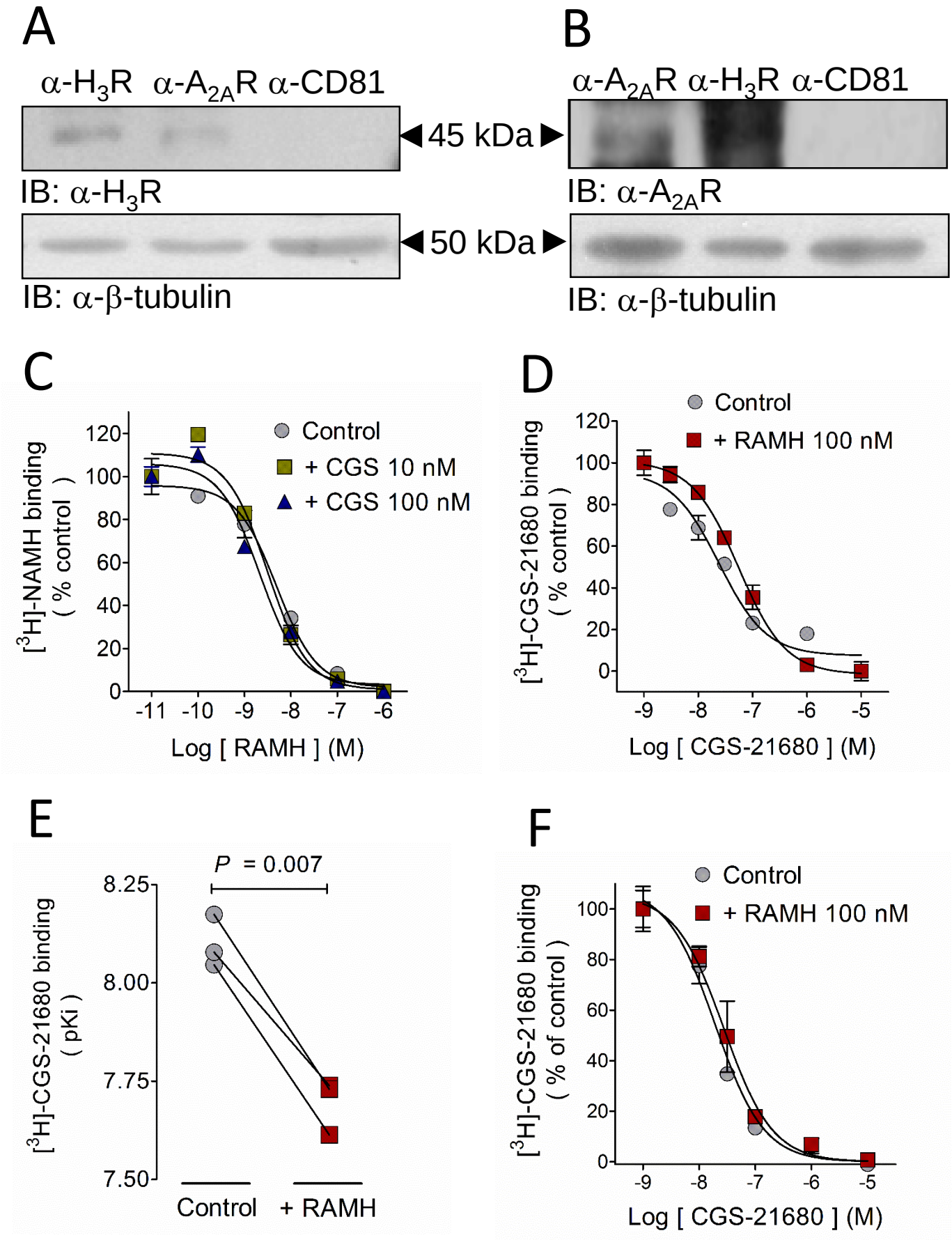
A
α-H3R α-A2AR α-CD81
45 kDa
IB: α-H3R
50 kDa
IB: α-β-tubulin
B
α-A2AR α-H3R α-CD81
IB: α-A2AR
IB: α-β-tubulin
C
[3H]-NAMH binding (% control)
Control
+ CGS 10 nM
+ CGS 100 nM
Log [RAMH] (M)
D
[3H]-CGS-21680 binding (% control)
Control
+ RAMH 100 nM
Log [CGS-21680] (M)
E
P = 0.007
[3H]-CGS-21680 binding (pKi)
Control
+ RAMH
F
[3H]-CGS-21680 binding (% of control)
Control
+ RAMH 100 nM
Log [CGS-21680] (M)